Title: Influence of cooling rate on structural and magnetic properties of (Fe78Nb8B14)1-xTbx alloys

Author: Grzegorz Ziółkowski, Artur Chrobak, Joanna Klimontko, Dariusz Chrobak, N. Randrianantoandro

Citation style: Ziółkowski Grzegorz, Chrobak Artur, Klimontko Joanna, Chrobak Dariusz, Randrianantoandro N. (2017). Influence of cooling rate on structural and magnetic properties of (Fe78Nb8B14)1-xTbx alloys. "AIP Advances" (Vol. 7, iss. 5 (2017), art. no. 056235, s. 1-6), doi 10.1063/1.4978698

Influence of cooling rate on structural and magnetic properties of $(Fe_{78}Nb_8B_{14})_{1-x}Tb_x$ alloys

G. Ziółkowski,[1,a] A. Chrobak,[1] J. Klimontko,[1] D. Chrobak,[2] and N. Randrianantoandro[3]
[1]*Institute of Physics, University of Silesia, Uniwersytecka 4, 40-007 Katowice, Poland*
[2]*Institute of Materials Science, University of Silesia, 75 Pułku Piechoty 1, 41-500 Chorzów, Poland*
[3]*Institut des Molécules et des Matériaux du Mans UMR CNRS 6283, LUNAM Université- Université du Maine, Avenue Olivier Messaien, 72085 Le Mans cedex 9, France*

(Presented 3 November 2016; received 23 September 2016; accepted 4 February 2017; published online 15 March 2017)

In the presented work we are focused on the influence of cooling rate on structural and magnetic properties of $(Fe_{78}Nb_8B_{14})_{1-x}Tb_x$ (x = 0.08, 0.1, 0.12) nanocrystalline bulk alloys. The samples were fabricated using the vacuum suction technique with different cooling rates controlled by different sample diameters (from 0.5 to 1.5 mm). The increased Nb content leads to the formation of specific microstructure and allows obtaining ultra-high coercive alloys just after casting without any additional treatment. The coercivity exceeds 8.6 T at the room temperature in case of optimal chemical and preparation conditions (x = 0.12, d = 0.5 mm) and 5.6 T for x = 0.1. The impact of Tb content as well as the cooling rate on magnetic and structural (XRD, SEM, MFM) properties is widely discussed in the context of reduction of rare earths in the RE-based permanent magnets. [http://dx.doi.org/10.1063/1.4978698]

INTRODUCTION

It is well known that hard magnetic materials are widely used in various fields of technical industry. Nowadays, ternary compounds of type Nd-Fe-B are considered as the best. Indeed, the value of coercive field is of about 1.2 T and the parameter $|BH|_{max}$ can reach values of about 400 kJ/m^3. Unfortunately, high content of rare earth (RE) additions implicates high price. On the other hand, the hard ferrite magnets are good economic alternative, however with relatively low maximum energy product (< 38 kJ/m^3). Therefore, especially important challenge in the field of the permanent magnets is to fill the gap between this alloys.[1] One can notice a trend towards searching new hard magnetic materials with a reduced content of rare earth elements or some other systems free of these ingredients with $|BH|_{max}$ parameter in order of 100-200 kJ/m^3, which should be sufficient for many applications.[2–13] It seems that the best solution of this challenge may be the composites of soft and hard magnetic phases. In this case, strong exchange interactions between magnetic moments associated with the different phases can leads to the so-called spring-magnetism, and in a consequence, combination of high magnetic remanence as well as maximum energy product. The key element in that way is developing of extremely hard magnetic material as a source of high coercivity for these kind of composites. In the case of such materials, important meaning has $|JH|_{max}$ parameter (where J is the magnetic polarization, equal to $\mu_0 M$) which describe the magnetic energy density stored into material and is related to the energy required for its demagnetization.

[a]Corresponding author: gziolkowski@us.edu.pl

Recently, we have reported ultra-high coercivity of Fe-Nb-B-RE (6 at. % of Nb) bulk nanocrystalline alloys produced by the vacuum suction casting technique, i.e. more than 7 T at the room temperature and after some field annealing.[14] It should be underlined that in the field of bulk materials this is a unique feature, giving new opportunities to designing new magnetic materials, including the mentioned composites. It was shown that the examined alloys contain some ultra-hard magnetic objects that do not directly contribute to the magnetization processes but, via direct interactions, influence magnetic characteristics of the whole alloy. The key point for understanding the magnetic hardening effect is a formation of specific microstructure controlled by the technology parameters (cooling rate) and a proper Nb content as an agent causing slowing down of crystallization during casting. Such alloys can not have high magnetic saturation and, in a consequence, remanence and the $|BH|_{max}$ parameter, due to the antiferromagnetic coupling between the Fe and Tb magnetic moments. However, the material with ultra-high coercivity can be an important addition in spring-exchange magnets.

Based on the previously obtained results,[14,15] it seems that an increase of cooling rate with a fixed Niobium concentration may leads to further improvements of coercivity, and therefore, should be additionally investigated. Moreover, it is worth to check how a decrease of Tb content influences the desired magnetic properties.

The aim of this work is to study an influence of cooling rate and Tb content on structural and magnetic properties of the $(Fe_{78}Nb_8B_{14})_{1-x}Tb_x$ ($x = 0.08, 0.1, 0.12$) bulk nanocrystalline alloys which have a potential to be a base for a new type of spring-exchange composites.

EXPERIMENTAL PROCEDURE

The series of bulk alloys $(Fe_{78}Nb_8B_{14})_{1-x}Tb_x$ (x = 0.08, 0.1, 0.12) where prepared using the vacuum suction casting technique[16] in the form of rods. The proper chemical compositions were obtained by weighting the amorphous base of $Fe_{78}Nb_8B_{14}$ with Tb. The cooling rate was controlled by the different sample diameter $d = 0.5$ mm, 1 mm and 1.5 mm. Structural observation were carried out using: a) X-ray diffraction by Siemens D-5000 diffractometer ($\theta - \theta$ configuration) with CuK_α radiation (1.5418 Å, 40 kV, 30 mA) without monochromator and with nickel filter, as well as b) Scanning electron microscopy (before this measurements the samples were cut, included into a resin and mechanical polished), and c) Quesant Q-Scope 250 AFM/MFM system, equipped with a 40 μm × 40 μm piezo-scanner. Finally, the magnetic hysteresis loops where measured, at room temperature, by the SQUID magnetometer (XL-7, Quantum Design). In all cases, the external magnetic field was applied along the rod axis.

RESULTS AND DISCUSSION

In order to determine crystalline phase compositions, the XRD measurements were performed for all studied alloys. Figure 1 shows XRD patterns obtained for the $(Fe_{78}Nb_8B_{14})_{1-x}Tb_x$ (x = 0.08, 0.1, 0.12) alloys with 1.5 mm in diameter. The alloys consist mainly hard magnetic phase $Tb_2Fe_{14}B$, relatively soft magnetic $TbFe_2$ and other phases like Fe_2B, FeO, Fe_2O_3, Nb-Fe-B. The highest contribution of the hard magnetic ternary phase (up to 90%) was noted in case of 10 and 12 at. % of Tb content. For $x = 0.08$ a significant decrease of the $Tb_2Fe_{14}B$ phase and increase of borides formation were observed. It should be noted that the XRD analysis performed for the alloys with different diameters ($d = 0.5$ mm, 1 mm and 1.5 mm) do not manifest any remarkable differences in the phase compositions. Table I summarizes selected values, resulting from the XRD patterns presented in Figure 1. Moreover, one may note that the sizes of the main phase grains (estimated based on the Scherrer equation) are in order of tens nm.

Figures 2a and 2b present comparison of microstructures (SEM) for the $(Fe_{78}Nb_8B_{14})_{0.88}Tb_{0.12}$ alloys prepared by the mold with $d = 0.5$ mm (a) and 1.5 mm (b). One may note that dependently on the cooling rate a specific microstructure is formed. In the case of $d = 0.5$ mm (the highest cooling rate), a formation of dendrite-like grains with micrometric (or even smaller) dimensions is clearly visible. An EDS analysis reveals that the grains (bright area) contain Fe and Tb, surely forming the hard magnetic $Tb_2Fe_{14}B$ phase. The dark areas contain increased concentration of

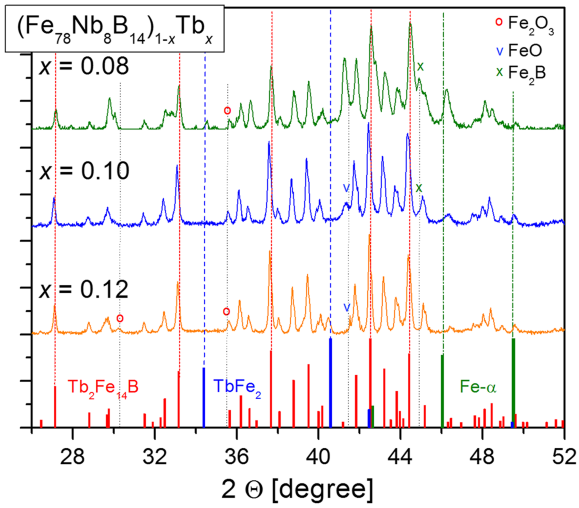

FIG. 1. The X-ray patterns for the $(Fe_{78}Nb_8B_{14})_{1-x}Tb_x$ (x = 0.08, 0.1, 0.12) alloys with 1.5 mm in diameter.

TABLE I. The phase analysis of the $(Fe_{78}Nb_8B_{14})_{1-x}Tb_x$ (x = 0.08, 0.1, 0.12) alloys with 1.5 mm in diameter.

x	$Tb_2Fe_{14}B$ [%] ±2	$TbFe_2$ [%] ±2	Fe_2B, FeO, Fe_2O_3, Nb-Fe-B [%] ±2	Unit cell [Å]	grain size [nm] ±10
0.08	63	5	32	a= 8.757 ±0.001, c=12.034 ±0.002	36
0.1	89	-	11	a= 8.779 ±0.001, c=12.068 ±0.001	40
0.12	85	3	12	a=8.771 ±0.001, c=12.054 ±0.002	47

non-magnetic Nb. For the alloy prepared with the lowest cooling rate (d = 1.5 mm), mainly a flat surface is observed, showing large grain with homogeneously dispersed Nb. The later is also confirm by the fact that in XRD pattern any Bragg's peaks, related to crystalline Nb, were not observed.

The different mictrostructures have an influence on magnetic domains. Figure 2 shows also topological AFM (c, d) and magnetic MFM (e, f) pictures for the $(Fe_{78}Nb_8B_{14})_{0.88}Tb_{0.12}$ alloys with 0.5 mm (left) and 1.5 mm (right) in diameter. In both cases the domain structure is irregular but, in the case of d = 0.5 mm it is more fragmented which is attributed to the dendrite grains revealed by the SEM observations.

The magnetic hysteresis loops for the selected alloys were presented in Figure 3. The comparison consist of three deferent cooling rates for optimal chemical composition (x = 0.12, the highest coercivity), as well as, three deferent chemical compositions for optimal cooling rate (d = 0.5 mm). Moreover, summary of important magnetic parameters for all studied materials were listed in Table II and graphically presented in Figure 4. It can be seen that the coercivity strongly increases with decreasing sample diameter as well as increasing of Tb content. Note, in the case of alloy with the low Terbium addition (8 at. %), the coercivity is still relatively high and equals 1.23 T for d = 1 mm. The strongest magnetic hardening effect was observed for the alloys with x = 0.1 i.e., coercive field increases from 1.16 T up to 5.6 T for diameter d = 1.5 mm and 0.5 mm, respectively. Important meaning has also $|JH|_{max}$ parameter which increases form 62 kJ/m^3 up to 700 kJ/m^3. Similar tendency can be seen in the case of material with optimal chemical composition (x = 0.12), however the hysteresis loop is opened and strongly asymmetric. Such situation suggests that coercivity may be much higher. Indeed, the $(Fe_{78}Nb_8B_{14})_{0.88}Tb_{0.12}$ alloy with d = 0.5 mm was chosen for further investigation in external magnetic field up to 14 T, presented as the inset in Figure 3. In this case the hysteresis loop is almost symmetric and the determined coercivity is equal to 8.6 T.

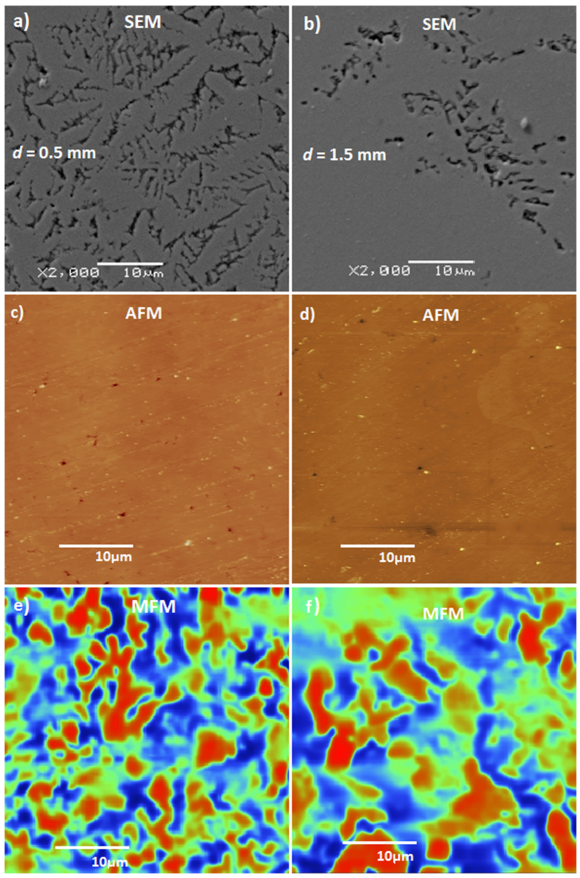

FIG. 2. The SEM and AFM/MFM images for the $(Fe_{78}Nb_8B_{14})_{0.88}Tb_{0.12}$ alloys with 0.5 mm (left column) and 1.5 mm (right column) in diameter. Note, the regions selected for SEM and AFM/MFM are not the same.

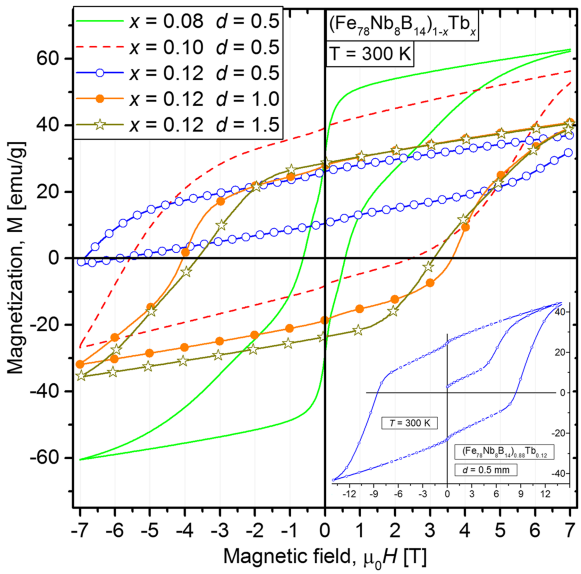

FIG. 3. The magnetic hysteresis loops for the $(Fe_{78}Nb_8B_{14})_{1-x}Tb_x$ (x = 0.08, 0.1, 0.12) alloys with different diameters, as well as the $(Fe_{78}Nb_8B_{14})_{0.88}Tb_{0.12}$ alloy with d = 0.5 mm measured up to 14 T (see the inset).

TABLE II. Selected magnetic parameters for the all studied samples (measurement error is in order of the last digit).

x	d [mm]	M_S [emu/g]	M_R [emu/g]	$\mu_0 H_{c-}$ [T]	$\mu_0 H_{c+}$ [T]	$\|JH\|_{max}$ [kJ/m^3]	$\|BH\|_{max}$ [kJ/m^3]
0.08	**0.5**	62.5	30	0.63	0.55	35	11
0.08	**1**	55	27.5	1.23	0.99	47	9.8
0.08	**1.5**	50	17	0.21	0.19	5	2.5
0.1	**0.5**	56.2	39	5.6	2.51	700	29.5
0.1	**1**	40	25	1.8	1.65	127	12
0.1	**1.5**	35.5	21.5	1.16	1.13	62	8.7
0.12	**0.5**	37	25.8	6.9	-	590	13.3
0.12	**1**	41	28	4.1	3.61	408	15
0.12	**1.5**	40.6	28.7	3.66	3.1	340	16.1

Let's analyze the M(H) curves. Especially interesting is the opened and asymmetric hysteresis loop for the $(Fe_{78}Nb_8B_{14})_{0.88}Tb_{0.12}$ alloy with d = 0.5 mm measured up to 7 T, in a contrast to almost fully symmetric hysteresis measured in higher range of external magnetic field up to 14 T. This observation indicates an appearing of some ultra-hard magnetic objects that do not change magnetization direction even in 7 T magnetic field. Interactions between these objects and the rest volume can cause the observed hysteresis shape. Moreover, the applied different cooling rates significantly change magnetic properties but do not influence phase structure. Therefore, the source of ultra-hard magnetic objects should be attributed to microstructure. Indeed, this conclusion is strongly supported by the SEM and MFM observations. In the case of sample with d = 1.5 mm the magnetic domains are rather smooth and regular in shape, while for the sample with d = 0.5 mm they are smallest and ragged. It should be noted that the great role in forming of such structure plays Niobium as agent causing slowing down of crystallization during casting. The specific microstructure, as an additional source of magnetic anisotropy, are responsible for the "disordered" magnetic domain structure. Finally, the highest observed coercivity is equal to 8.6 T at room temperature and without any additional treatment, which classifies this material as perfect candidate for developing of permanent magnets based on ultra-high coercive additions.

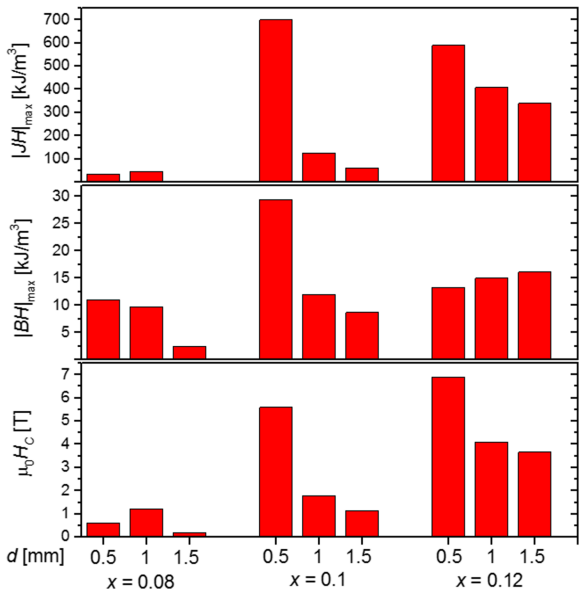

FIG. 4. Summary of the magnetic parameters for the all studied alloys type of $(Fe_{78}Nb_8B_{14})_{1-x}Tb_x$ with different diameters.

CONCLUSIONS

The main conclusions of this work can be summarized as follows:

- In the case of the studies alloys, the increase of the cooling rate leads to the magnetic hardening effect. The desired parameters (i.e. coercivity, $|JH|_{max}$ and $|BH|_{max}$) increases, reaching the maximum values: H_c=6.9 T for x=0.12 and d=0.5 mm, $|JH|_{max}$= 700 kJ/m^3 and $|BH|_{max}$= 29.5 kJ/m^3 for x=0.1 and d=0.5 mm.
- In a contrast to similar alloys with lower Nb content i.e. $(Fe_{80}Nb_6B_{14})_{1-x}Tb_x$, the 8 at. % is sufficient to obtain coercivity higher than 7 T but without field annealing. The ultra-high coercivity is related to the formed low dimensional dendrite microstructure.
- The $(Fe_{78}Nb_8B_{14})_{0.9}Tb_{0.10}$ alloy prepared with 0.5 mm in diameter can be consider as ultra-high coercive magnet ($|JH|_{max}$ = 700 kJ/m^3, H_C = 5.6 T) with reduced RE content.

ACKNOWLEDGMENTS

This work was supported by National Science Centre in Poland by the grant 2015/19/B/ST8/02636.

[1] J. M. D. Coey, Scripta Materialia **67**, 524 (2012).
[2] N. Poudyal and J. P. Liu, J. Phys. D: Appl. Phys. **46**, 23 (2013).
[3] R. M. Liu, M. Yue, R. Na, Y. W. Deng, D. T. Zhang, W. Q. Liu, and J. X. Zhang, J. Appl. Phys. **109** (2011).
[4] F. E. Luborsky, J. Appl. Phys. **37**, 1091 (1966).
[5] J. J. Croat, J. F. Herbst, R. W. Lee, and F. E. Pinkerton, J. Appl. Phys. **55**, 2078 (1984).
[6] M. Sagawa, S. Fujimura, H. Yamamoto, and Y. Matsuura, IEEE. T. Magn. **20**(5), 1584 (1984).
[7] N. Randrianantoandro, A. D. Crisan, O. Crisan, J. Marcin, J. Kovac, J. Hanko, J. M. Grenèche, P. Svec, A. Chrobak, and I. Skorvanek, J. Appl. Phys. **108** (2010).
[8] T. Kulik, J. Non-Cryst. Solids **287**, 145 (2001).
[9] H. Kronmuller and M. Fahnle, Cambridge University Press, 2003.
[10] L. Zhou, M. K. Miller, P. Lu, L. Ke, R. Skomski, H. Dillon, Q. Xing, A. Palasyuk, M. R. McCartney, D. J. Smith, S. Constantinides, R. W. McCallum, I. E. Anderson, V. Antropov, and M. J. Kramer, Acta Mater. **74**, 224 (2014).
[11] J. Zhang, K. Y. Lim, Y. P. Fenga, and Y. Li, Scripta Mater. **56**, 943 (2007).
[12] J. Liu, H. Sepehri-Amin, T. Ohkubo, K. Hioki, A. Hattori, T. Schrefld, and K. Hono, Acta Mater. **82**, 336 (2015).
[13] J. M. D. Coey, *Magnetism and Magnetic Materials*, Cambridge University Press, 2010.
[14] A. Chrobak, G. Ziółkowski, N. Randrianantoandro, J. Klimontko, D. Chrobak, K. Prusik, and J. Rak, Acta Materialia **98**, 318 (2015).
[15] A. Chrobak, G. Ziółkowski, and N. Randrianantoandro, J. Alloys Comp. **583**, 48 (2014).
[16] A. Chrobak, M. Karolus, and G. Haneczok, Solid State Phenomena **163**, 233 (2010).